



Are benthic nutrient fluxes from intertidal mudflats driven by surfaced sediment characteristics?

Justine Louis, Laurent Jeanneau, Françoise Andrieux-Loyer, Gérard Gruau, Florian Caradec, Nathalie Le Bris, Marion Chorin, Emilie Jardé, Emilie Rabiller, Christophe Petton, et al.

► To cite this version:

Justine Louis, Laurent Jeanneau, Françoise Andrieux-Loyer, Gérard Gruau, Florian Caradec, et al.. Are benthic nutrient fluxes from intertidal mudflats driven by surfaced sediment characteristics?. *Comptes Rendus. Géoscience*, 2021, 353 (1), pp.173-191. <10.5802/crgeos.57>. <insu-03229725>

HAL Id: insu-03229725

<https://insu.hal.science/insu-03229725v1>

Submitted on 19 May 2021

HAL is a multi-disciplinary open access archive for the deposit and dissemination of scientific research documents, whether they are published or not. The documents may come from teaching and research institutions in France or abroad, or from public or private research centers.

L'archive ouverte pluridisciplinaire **HAL**, est destinée au dépôt et à la diffusion de documents scientifiques de niveau recherche, publiés ou non, émanant des établissements d'enseignement et de recherche français ou étrangers, des laboratoires publics ou privés.



Distributed under a Creative Commons CC BY 4.0 - Attribution - International License



INSTITUT DE FRANCE
Académie des sciences

Comptes Rendus

Géoscience

Sciences de la Planète


Justine Louis, Laurent Jeanneau, Françoise Andrieux-Loyer, Gérard Gruau, Florian Caradec, Nathalie Lebris, Marion Chorin, Emilie Jardé, Emilie Rabiller, Christophe Petton, Guillaume Bouger, Patrice Petitjean and Anniët M. Laverman

Are benthic nutrient fluxes from intertidal mudflats driven by surface sediment characteristics?

Volume 1, issue 0 (0000), p. 000-000

[<https://doi.org/10.5802/crgeos.57>](https://doi.org/10.5802/crgeos.57)

© Académie des sciences, Paris and the authors, 2021.
Some rights reserved.

 This article is licensed under the
CREATIVE COMMONS ATTRIBUTION 4.0 INTERNATIONAL LICENSE.
<http://creativecommons.org/licenses/by/4.0/>



*Les Comptes Rendus. Géoscience — Sciences de la Planète sont membres du
Centre Mersenne pour l'édition scientifique ouverte
www.centre-mersenne.org*



Original Article — Hydrology, Environment

Are benthic nutrient fluxes from intertidal mudflats driven by surface sediment characteristics?



Justine Louis^{*,a}, Laurent Jeanneau^b, Françoise Andrieux-Loyer^c, Gérard Gruau^b, Florian Caradec^c, Nathalie Lebris^a, Marion Chorin^a, Emilie Jardé^b, Emilie Rabiller^c, Christophe Petton^b, Guillaume Bouger^a, Patrice Petitjean^b and Annet M. Laverman^a

^a Centre National de la Recherche Scientifique (CNRS), ECOBIO – UMR 6553, Université de Rennes 1, 35042 Rennes, France

^b Centre National de la Recherche Scientifique (CNRS), Géosciences Rennes – UMR 6118, Université de Rennes 1, 35042 Rennes, France

^c Ifremer, DYNECO PELAGOS, ZI Pointe du Diable, 29280 Plouzané, France

E-mails: justine.louis@univ-rennes1.fr (J. Louis), laurent.jeanneau@univ-rennes1.fr (L. Jeanneau), Francoise.Andrieux@ifremer.fr (F. Andrieux-Loyer), gerard.gruau@univ-rennes1.fr (G. Gruau), Florian.Caradec@ifremer.fr (F. Caradec), nathalie.lebris@univ-rennes1.fr (N. Lebris), marion.chorin@univ-rennes1.fr (M. Chorin), emilie.jarde@univ-rennes1.fr (E. Jardé), Emilie.Rabiller@ifremer.fr (E. Rabiller), christophe.petton@univ-rennes1.fr (C. Petton), guillaume.bouger@univ-rennes1.fr (G. Bouger), patrice.petitjean@univ-rennes1.fr (P. Petitjean), annet.laverman@univ-rennes1.fr (A. M. Laverman)

Abstract. A broad sampling program was carried out in the spring of 2019 on the Brittany coast to assess how the surface sediment characteristics drive the benthic effluxes of ammonium (NH_4^+) and phosphate (PO_4) from intertidal mudflats. A total of 200 sediment samples were characterized by their porosity, grain-size, elemental composition and pigment contents, as well as the benthic fluxes of NH_4^+ and PO_4 determined by core incubations. The results showed that (1) a high phaeopigment and iron-bound phosphorus content (Fe-P) and a low porosity were significantly related to the high PO_4 flux, and (2) a high porosity and the TN:Org-P ratio in the sediment organic matter (SOM) were related to the high NH_4^+ flux. This indicated that PO_4 fluxes would be more driven by the redox status of the sediment through the desorption of Fe-P under specific anoxic conditions during the algal decomposition. NH_4^+ fluxes would be more driven by high NH_4^+ recycling rates from SOM mineralization and high sediment–water exchanges, enhancing the diffusion of NH_4^+ to the overlying water. The present study allowed to highlight the large variability in the benthic nutrient fluxes at the regional scale, as a result of the connections between microbial (SOM mineralization), chemical (adsorption–desorption) and physical (diffusion) processes.

Keywords. Benthic nutrient fluxes, Coastal sediment, Organic matter, Spatial variability, Diffusive transport, Microbial and chemical processes.

Manuscript received 14th December 2020, revised 31st March 2021, accepted 27th April 2021.

* Corresponding author.

1. Introduction

Eutrophication is the process by which nutrients, mostly nitrogen (N) and phosphorus (P), accumulate in a body of water, as defined by Smith *et al.* [1999]. A typical result of coastal eutrophication is the growth of dense macroalgal mats observed in shallow waters worldwide near industrial, agricultural and urban areas [Gladyshev and Gubelit, 2019, Morand and Briand, 1996, Valiela *et al.*, 1997]. This phenomenon was given the evocative name “green tides” because of the visible proliferation of *Ulva sp.* in both estuarine and coastal marine ecosystems [Perrot *et al.*, 2014, Pinay *et al.*, 2018]. The subsequent decay of the macroalgal biomass has harmful environmental consequences through changes in the microbial and macrofaunal food web in the sediment [Davoult *et al.*, 2017, García-Robledo *et al.*, 2008, Hardison *et al.*, 2013, Valiela *et al.*, 1997] and an accumulation of toxic hydrogen sulfide [Nedergaard *et al.*, 2002]. Even though river nutrient loading, especially N, is the main cause of green tides [e.g. Perrot *et al.*, 2014], coastal sediments could be an additional source of nutrients for macroalgae, thus contributing to eutrophication [Sundbäck *et al.*, 2003, Engelsén *et al.*, 2008, Robertson and Savage, 2018]. For example, it has been shown that benthic nutrient effluxes could supply up to 55–100% and 30–70% of the N and P requirement, respectively, needed to initiate the growth of filamentous green algal mats in shallow microtidal embayments on the west coast of Sweden [Sundbäck *et al.*, 2003].

In order to improve our understanding of coastal eutrophication, mathematical models have been developed by coupling hydro-biogeochemical and ecological mechanisms [Le Moal *et al.*, 2019 and references therein]. Models such as the “Mars-Ulves” [Perrot *et al.*, 2014] and “ECO-MARS3D” models [Ménesguen *et al.*, 2019] predict fine-scale algal blooms based on nutrient loading from rivers, pelagic nutrient cycling and the primary production of a coastal system, whereas the benthic compartment is represented in less detail. Currently, a constant benthic flux of N and P is used to take the nutrient exchanges between the sediment and bottom waters into account, but this remains limited due to the lack of suitable data for a given area. Determining the spatial variability of the benthic nutrient fluxes requires a large analytical effort, and may be high according

the variations of environmental factors (e.g. hydrodynamism, anthropogenic pressures) of coastal ecosystems. This could be facilitated by using sedimentary proxies, which are easily measurable and directly related to benthic fluxes.

Benthic N and P fluxes, through the regeneration of ammonium (NH_4^+) and phosphate (PO_4) in the sediment, are driven by chemical (e.g. adsorption), biological (e.g. mineralization) and physical (e.g. diffusion) processes. To a large extent, they depend on (1) the redox conditions, (2) the deposition rate and the composition of the sedimentary organic matter (SOM), and (3) the physical properties of the sediment [e.g. Ait Ballagh *et al.*, 2020, Arndt *et al.*, 2013, Dauwe *et al.*, 2001 and references therein; Khalil *et al.*, 2018, Middelburg *et al.*, 1996]. Redox conditions, driven by electron acceptor availability in the porewater, control the microbially mediated processes in N and P cycling [Capone *et al.*, 2008 and references therein; Paytan and McLaughlin, 2007, Sundby *et al.*, 1992] and the adsorption–desorption processes of PO_4 onto iron oxides [Andrieux-Loyer *et al.*, 2008, 2014, Krom and Berner, 1980, Rozan *et al.*, 2002].

The composition of SOM is influenced by a mixture of organic matter (OM) inputs from both autochthonous (e.g. microphytobenthos and sediment-attached bacteria) and allochthonous sources (e.g. algal and vascular plant detritus from terrestrial and marine origins). It is generally accepted that a high contribution of algal biomass relative to terrestrial detritus in the SOM composition enhances its biodegradability [e.g. Arndt *et al.*, 2013]. Two markers can be used to assess the labile OM flux in sediment: the chl_a and phaeopigment contents in surface sediment. They are good tracers of OM produced by photosynthetic organisms [Dell’Anno *et al.*, 2002]. Whereas the chl_a content in surface sediment would be mainly related to the microphytobenthos biomass, the content of its breakdown product, phaeopigment, would indicate the sedimentation of phytoplankton and macroalgal detritus from the water column [Therkildsen and Lomstein, 1993].

The SOM composition may also be characterized by the elemental C:N:P ratios. The C:N ratio is widely used to discriminate the sources of OM in the surface sediment [e.g. Dubois *et al.*, 2012, Galois *et al.*, 2000, Gu *et al.*, 2017]. Typically, C:N values > 20 can be used to distinguish terrestrial higher plants

from macrophytes (from 10 to 20) and phytoplankton (from 6 to 10) [Dubois *et al.*, 2012, Liénart *et al.*, 2017, Meyers, 1994]. Therefore, it is assumed that when the C:N ratio is lower, the organic matter is more easily biodegradable [Enríquez *et al.*, 1993]. Conversely, the N:P ratio in SOM is not commonly used to describe the origin and biodegradability of SOM. Nevertheless, an increase in the N:P ratio in the surface sediment could reflect the enrichment of OM via the decay of macroalgae, as observed in the eutrophic lagoon of Venice [Sfriso *et al.*, 1988].

Physical sediment properties, such as the grain-size distribution and porosity, also affect SOM mineralization and the transport processes of solutes, and thus benthic fluxes. Fine-grained sediment, reflecting a high proportion of clay minerals, may prevent the microbially mediated OM degradation through a physical protection of the OM [e.g. Arndt *et al.*, 2013 and references therein; Rasheed *et al.*, 2003]. Porosity, which is generally inversely related to grain-size [Meade, 1966], is a key parameter driving the sediment–water exchanges of solutes, including diffusion, advection and bio-irrigation [Boudreau, 1996, 1997]. Therefore, a high porosity could, for example, enhance the diffusive fluxes across the sediment–water interface.

The present study was based on the hypothesis that benthic nutrient fluxes may be directly related to the sedimentary characteristics. Two previous studies carried out in temperate estuaries showed relationships between NH_4^+ / PO_4 fluxes and markers of the SOM composition [Clavero *et al.*, 2000, Cowan and Boynton, 1996]. The nutrient fluxes were positively correlated with the chl *a* content along the axis of Chesapeake Bay, USA [Cowan and Boynton, 1996], and negatively correlated with the C:N ratio in the seasonal study carried out in the Palmones River estuary in southern Spain [Clavero *et al.*, 2000]. Therefore, the C:N ratio and chl *a* content may be effective proxies of the NH_4^+ and PO_4 fluxes. However, the sedimentary characteristics were not ranked in these previous studies, and the effects of the environmental conditions (e.g. the temperature of bottom water), known to affect both the diffusion and metabolic activities of benthic bacteria [Arndt *et al.*, 2013 and references therein], were not discerned from those of the SOM composition [Clavero *et al.*, 2000].

The aim of the present study was to investigate the relationships between benthic nutrient fluxes and

the surface sediment characteristics from intertidal mudflats. Our objective was to answer the following questions: (1) What are the main drivers of benthic nutrient fluxes? (2) Are these drivers similar with regards to the NH_4^+ and PO_4 fluxes? (3) Does the SOM composition have a predominant role compared to the physical properties of the sediment, and (4) Can the sedimentary properties be used as efficient tools to predict NH_4^+ and PO_4 fluxes?

To this end, a broad sediment sampling campaign was carried out in the spring of 2019 on the Brittany coast (France). Since the 1970s, the Brittany coast has been particularly affected by green tides; this timeline coincides with changes in agricultural practices and an increase in anthropogenic nitrogen loading in the watersheds [Morand and Briand, 1996]. Many surface and subsurface waters in Brittany have nitrate concentrations which exceed the European Community 50 $\text{mg}\cdot\text{L}^{-1}$ drinking standard.

A total of 200 sediment samples collected from 45 sites were analyzed for their NH_4^+ and PO_4 fluxes as well as their physical properties and chemical composition. This sampling strategy allowed to investigate a range of sedimentary characteristics while maintaining similar climatic conditions. The surface sediments were characterized by their porosity and grain-size, as well as their carbon, nitrogen, total phosphorus, chl *a* and phaeopigment contents. In addition, organic phosphorus (Org-P) and iron oxide-bound phosphorus (Fe-P) were distinguished from the total phosphorus pool.

2. Materials and methods

2.1. Study sites and sampling

The study sites were located in macrotidal mudflats in Brittany (north-western France) under eutrophic conditions where green algae mats are observed (<https://bretagne-environnement.fr/donnees-algues-vertes-bretagne>). The mudflats that we selected for our study are the mudflats that are regularly monitored as part of the green tide monitoring programs set up by the Loire-Bretagne Water Agency (CEVA, final report, 2015). Over the sampling period (between mid-April to mid-June 2019), the tidal range fluctuated from 2 to 9 m. Overall, 200 sediment samples were collected from 45 sites (Figure 1, Table S1) at mid–low tide. Sediment cores were sampled with a PVC core (diameter = 6 cm,

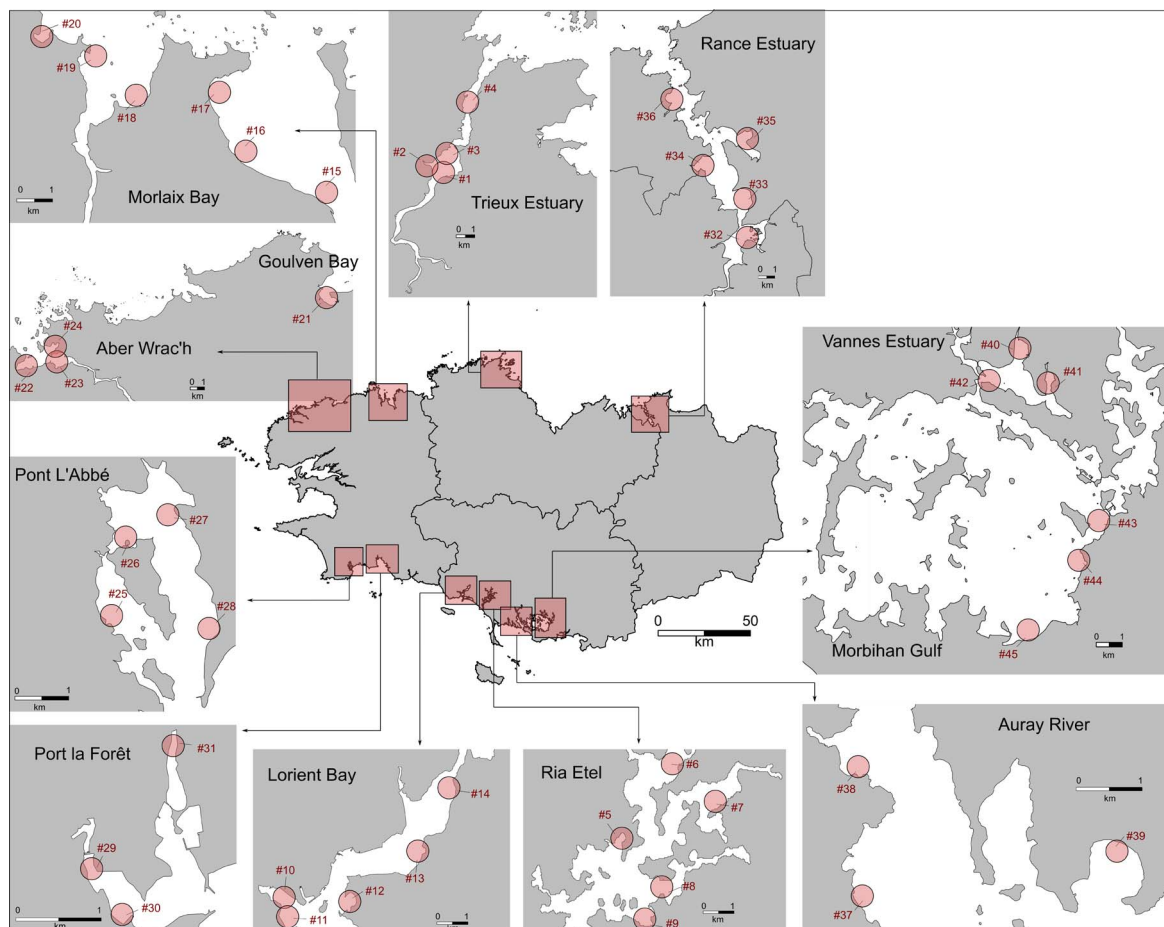


Figure 1. Location of mudflats ($n = 12$) and sites of sampling ($n = 45$) in spring (April until June) 2019. See the list of sites and sampling plan in Supplementary annex Table 1.

$h = 20$ cm) in the upper 10 cm sediment layer for the benthic flux measurements, and another core (diameter = 9 cm, $h = 5$ cm) was sampled in order to analyze the surface sediment characteristics (Figure S1). For the benthic flux measurements, the cores were incubated in the dark directly on site in a mobile laboratory under controlled temperature (19 ± 2 °C) within one hour following sampling (see below). Based on the sample collected using the PVC core with a height of 5 cm, an aliquot of the wet sediment, with a known volume and weight, was maintained at 4 °C and used to determine the porosity. The remaining sediment was frozen at -20 °C in order to analyze the pigment content (chl a and phaeopigment), phosphorus speciation, elemental composition and grain-size.

2.2. Benthic fluxes

The cores were incubated in the dark during 4 hours for the NH_4^+ and PO_4 efflux measurements. The overlying water was replaced by 150 mL of nutrient-free artificial seawater ($[\text{NaCl}] = 33 \text{ g}\cdot\text{L}^{-1}$, $[\text{NaHCO}_3] = 0.2 \text{ g}\cdot\text{L}^{-1}$, $\text{pH} \approx 8$) and gently aerated by bubbling in order to preserve the redox conditions of the sediment. Two $0.2 \mu\text{m}$ -filtered water samples were collected in the overlying water after 2 h and 4 h of incubation and stored at refrigerator temperature (4 °C) for less than three days prior to the nutrient analysis. The NH_4^+ , PO_4 , NO_2^- and NO_3^- concentrations in the overlying water were measured with the colorimetric method using an automated photometric analyzer Gallery™, with a detection limit of 0.9, 0.2,

0.07 and 3.6 μM , respectively. All of the NO_2^- and NO_3^- concentration measurements were below the detection limit.

The NH_4^+ and PO_4 fluxes across the sediment–water interface were accessed by using the change in the molar concentration of the solute in the known volume of overlying water as a function of incubation time and the surface area of the sediment core [Aller *et al.*, 1985]. If the rate of nutrient release from the sediment did not follow a linear trend over the incubation period, only the first sample was considered in the flux estimation. This was the case for PO_4 when the exchanges between the sediment and water reached an equilibrium state after two hours of incubation, in general, due to the re-adsorption onto particles [Sundby *et al.*, 1992]. Note that these fluxes were conducted under standardized conditions (temperature, aeration) and therefore considered as potential fluxes.

All of the values are reported in Supplementary Table S1.

2.3. Analysis of the sedimentary characteristics

The porosity was calculated by drying a previously weighed wet aliquot sediment at 60 °C. The water loss, determined by mass difference, and the sediment density set at 2.55 were used to calculate the porosity [Krom and Berner, 1980]. The particle-size distribution (<2 mm) was measured using a laser diffraction instrument (Malvern Mastersizer). The particles were classified as either sand (63–2000 μm), silt (3–63 μm) or clay (<3 μm) fractions [e.g. Keil and Hedges, 1993, Pye and Blott, 2004]. “Mud” is defined as the sum of the clay and silt particles. The percentage of mud was used as a sedimentary parameter thereafter.

The pigment content (chl *a* and phaeopigment) was measured in freeze-dried sediment (0.5–1 g) extracted in 90% acetone (10 mL) in the dark (18–20 h) at 4 °C. Each sample was previously gently ground using an agate pestle and mortar. After centrifugation, the chl *a* and phaeopigment contents were measured in the supernatant using the spectrophotometric method of Lorenzen [1967] at 665 and 750 nm (Uvikon spectrophotometer), and expressed in $\mu\text{g}\cdot\text{g}^{-1}$ of dry sediment. The detection limits of the chl *a* and phaeopigment contents were 2.7 and 12.9 $\mu\text{g}\cdot\text{g}^{-1}$, respectively.

The total organic carbon and nitrogen (TOC and TN) contents were determined using an element analyzer (FLASH™ 2000 OEA). An aliquot of freeze-dried and crushed sediment was acid-treated with 2N HCl to remove the carbonate and was subsequently rinsed with deionized water. After centrifugation, the carbonate-free sample was dried at 60 °C, and ground before being placed into a tin capsule for the TOC analysis. A second aliquot without an acidification treatment was used to determine the TN analysis.

The iron oxide-bound P (Fe-P) content was determined using a Dithionite-Bicarbonate solution [Ruttenberg, 1992], as described in Andrieux-Loyer *et al.* [2008]. The total P (P_{tot}) content was determined using a 1 mol·L⁻¹ HCl treatment overnight after sediment ignition at 550 °C (4 h), while the inorganic P content refers to the sum of the P-forms (Fe-bound P, Ca-bound P and detrital P), that was extracted with 1 mol·L⁻¹ HCl before sediment ignition [Aspila *et al.*, 1976]. The organic P (Org-P) content was then quantified by calculating the difference between the total P and inorganic P contents [Andrieux-Loyer *et al.*, 2008]. The phosphorus-form extracts were subsequently analyzed using segmented flow analysis (SFA) [Aminot and K  rouel, 2007]. The Org-P and Fe-P represented the pool of potentially bioavailable P.

The TOC, TN, P_{tot} , Org-P and Fe-P contents were expressed as the mass of the carbon, nitrogen and phosphorus in the total dry mass of the sediment.

The C:N and TN:Org-P ratios (mol:mol) in SOM were calculated from the TOC, TN and Org-P contents.

All of the values are reported in Supplementary Table S1.

2.4. Statistical analysis

Pearson's correlation matrix was calculated to establish the pairwise correlations between the sedimentary characteristics of the sediment. The relationships between the benthic nutrient fluxes and the sedimentary characteristics were assessed through multiple linear regressions. To better predict NH_4^+ and PO_4 fluxes, two models were built by multiple linear regression (MLR) using a stepwise selection procedure based on the Akaike information criterion (AIC). To ensure that the multi-collinearity did not skew our results, the variance inflation factors (VIF) were measured. None of the VIF values were higher

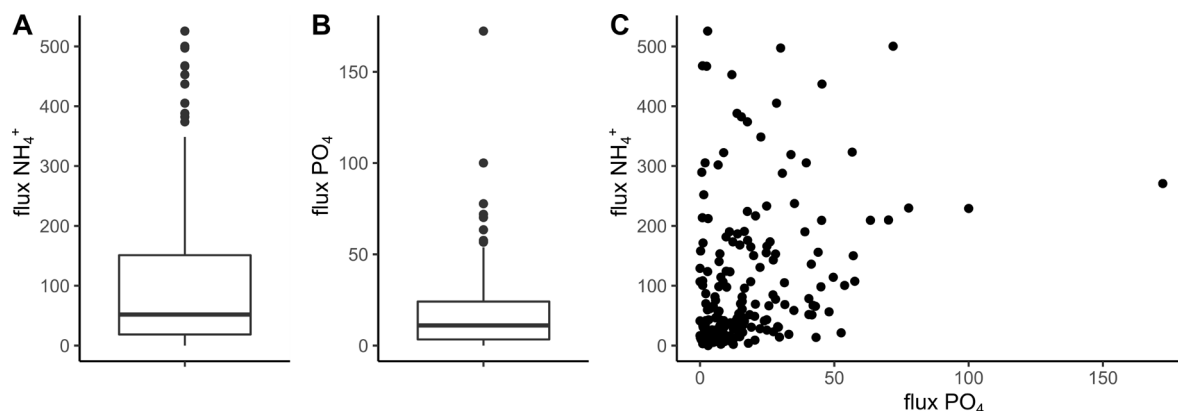


Figure 2. Boxplot of NH_4^+ (A) and PO_4 (B) effluxes, and NH_4^+ effluxes versus PO_4 effluxes (C) in $\mu\text{mol}\cdot\text{m}^{-2}\cdot\text{h}^{-1}$. Within the boxes, medians are the black lines. First and third quartiles are hinges, outliers are black dots.

than 3 (a threshold value was set at 5). In addition, when the selected variables had a Pearson's correlation higher than 0.7 between them, we checked that there was no interaction effect in the model. To identify the main drivers of the benthic nutrient fluxes by MLR, the data were normalized beforehand, and a p -value < 0.05 for the F -test was used to consider a significant effect of one predictor variable on the model. In addition to the calculation of AIC, the K-fold cross validation was run to evaluate the performance of each model built by linear regressions. The data set was split into 10 folds. In order to compare two means, a Student's t -test was performed when the sample size (n) was higher than 30. Each statistical analysis was performed using the R-studio software. The “aod”, “car” and “caret” packages were used to calculate AIC and VIF and to perform the k-fold cross validation, respectively. The “lm”, “step” and “scale” functions were used to perform the linear regressions, the stepwise selection procedure by MLR and the database normalization, respectively.

3. Results

3.1. Benthic nutrient fluxes

Taking the entire data set into account, the average NH_4^+ and PO_4 fluxes were $101 \pm 117 \mu\text{mol}\cdot\text{m}^{-2}\cdot\text{h}^{-1}$ and $17 \pm 20 \mu\text{mol}\cdot\text{m}^{-2}\cdot\text{h}^{-1}$, respectively. Over 50% of the NH_4^+ fluxes ranged from 19 and $151 \mu\text{mol}\cdot\text{m}^{-2}\cdot\text{h}^{-1}$, with values up to $526 \mu\text{mol}\cdot\text{m}^{-2}\cdot\text{h}^{-1}$ (Figure 2A).

With regards to the PO_4 fluxes, 50% of the data ranged from 3 and $24 \mu\text{mol}\cdot\text{m}^{-2}\cdot\text{h}^{-1}$, with a maximum flux of $172 \mu\text{mol}\cdot\text{m}^{-2}\cdot\text{h}^{-1}$ (Figure 2B). In general, the PO_4 fluxes were lower than those of NH_4^+ . Over 50% of the N:P flux ratios ranged from 2 to 12, with values up to 765. The large variability in the ratios of the N:P fluxes reflects a weak correlation between the NH_4^+ and PO_4 fluxes (Pearson's coefficient = 0.31, p -value < 0.05) (Figure 2C). The lowest N:P flux ratios ($\text{N:P} \leq 2$) were significantly explained by high PO_4 fluxes (mean = $25 \mu\text{mol}\cdot\text{m}^{-2}\cdot\text{h}^{-1}$) and low NH_4^+ fluxes ($31 \mu\text{mol}\cdot\text{m}^{-2}\cdot\text{h}^{-1}$) (Student's t -test for one sample, p -value < 0.05). The highest ratios for the N:P fluxes ($\text{N:P} \geq 12$) were significantly explained by low PO_4 fluxes (mean = $7 \mu\text{mol}\cdot\text{m}^{-2}\cdot\text{h}^{-1}$) and high NH_4^+ fluxes ($192 \mu\text{mol}\cdot\text{m}^{-2}\cdot\text{h}^{-1}$) (Student's t -test for one sample, p -value < 0.05) (Figure S2).

The variability of both NH_4^+ and PO_4 fluxes at the regional scale allowed to distinguish the locations where the sediment presented the highest average effluxes of nutrient. For the NH_4^+ effluxes, they were Gulf of Morbihan (mean: $185 \mu\text{mol}\cdot\text{m}^{-2}\cdot\text{h}^{-1}$), Vannes Estuary (mean: $173 \mu\text{mol}\cdot\text{m}^{-2}\cdot\text{h}^{-1}$) and Auray River (mean: $162 \mu\text{mol}\cdot\text{m}^{-2}\cdot\text{h}^{-1}$) (Figure 3). For the PO_4 effluxes, they were Lorient Bay (mean: $34 \mu\text{mol}\cdot\text{m}^{-2}\cdot\text{h}^{-1}$), Pont L'Abbé (mean: $30 \mu\text{mol}\cdot\text{m}^{-2}\cdot\text{h}^{-1}$) and Rance Estuary (mean: $30 \mu\text{mol}\cdot\text{m}^{-2}\cdot\text{h}^{-1}$) (Figure 4). By contrast, the three locations which presented the lowest average effluxes of NH_4^+ were Aber Wrac'h (mean: $19 \mu\text{mol}\cdot\text{m}^{-2}\cdot\text{h}^{-1}$), Morlaix Bay (mean: $48 \mu\text{mol}\cdot\text{m}^{-2}\cdot\text{h}^{-1}$) and Port

La Forêt (mean: $79 \mu\text{mol}\cdot\text{m}^{-2}\cdot\text{h}^{-1}$) (Figure 3), and those with the lowest average effluxes of PO_4^{3-} were Ria Etel (mean: $3 \mu\text{mol}\cdot\text{m}^{-2}\cdot\text{h}^{-1}$), Gulf of Morbihan (mean: $4 \mu\text{mol}\cdot\text{m}^{-2}\cdot\text{h}^{-1}$) and Port la Forêt (mean: $7 \mu\text{mol}\cdot\text{m}^{-2}\cdot\text{h}^{-1}$) (Figure 4). A high spatial variability of these fluxes was also observed between the sampling sites of the same location (Figures 3 and 4, Table S1). For example, in the Gulf of Morbihan, the lowest effluxes of NH_4^+ were measured at the site #45 ($7.3 \pm 1.4 \mu\text{mol}\cdot\text{m}^{-2}\cdot\text{h}^{-1}$), whereas the site #44 presented large effluxes of NH_4^+ ($388.6 \pm 189.5 \mu\text{mol}\cdot\text{m}^{-2}\cdot\text{h}^{-1}$) (Figure 3).

3.2. Surface sediment characteristics

The distribution and pairwise correlations with Pearson's coefficient for the surface sediment characteristics measured in the present study are presented in Tables 1 and 2.

The particle-size distribution of the samples indicates that the median grain-size (D50) ranged from 16 to 519 μm . With an average mud content of $68.3 \pm 17.2\%$ for all of the samples, the clay and silt particles represented 4.7 ± 2.1 and $63.6 \pm 15.4\%$ of the particle-size distribution, respectively. According to the ternary diagram based on the sand/mud ratios proposed by Flemming [2000], a large proportion of the surface sediments collected in the present study were classified as sandy mud (38%) and slightly sandy mud (49%). As expected, the mud content was positively correlated with the porosity of the sediment (Pearson's coefficient = 0.82, p -value < 0.05). The average porosity was $69.8 \pm 10.3\%$ with values that ranged from 46 to 87%.

The mud content was also positively correlated with the TOC (Pearson's coefficient = 0.64, p -value < 0.05), TN (Pearson's coefficient = 0.73, p -value < 0.05) and Org-P contents (Pearson's coefficient = 0.72, p -value < 0.05) in the surface sediment. The TOC, TN and Org-P contents averaged $2.2 \pm 1.2\%$, $0.24 \pm 0.12\%$ and $0.026 \pm 0.014\%$, respectively. With an average P_{tot} content of $0.055 \pm 0.022\%$, the amount of Org-P was $45 \pm 12\%$ of the P_{tot} content compared to $14 \pm 6\%$ for the Fe-P (average content of $0.008 \pm 0.005\%$).

The C:N and TN:Org-P ratios in the SOM averaged 10.0 ± 2.4 and 23.1 ± 6.9 , respectively. The C:N ratios reached up to 21.9 with half of the values ranging from 8.7 to 10.9. The highest values corresponded to

the sediment samples collected in the Goulven Bay (mean = 17.8 ± 3.9).

The accumulation of OM from the algal biomass (which included microphytobenthos, pelagic phytoplankton, macroalgae) in the surface sediment was described by the chl *a* and phaeopigment contents, with a mean value of 5.8 ± 4.8 and $28 \pm 18.7 \mu\text{g}\cdot\text{g}^{-1}$ of dry sediment, respectively. The chl *a* and phaeopigment contents were positively correlated with the TOC, TN and Org-P contents (Pearson's coefficient > 0.6, p -value < 0.05).

3.3. Relationships between the sedimentary parameters and benthic nutrient fluxes

The stepwise multiple linear regression (MLR) allowed to select the best combination of sedimentary characteristics to predict the NH_4^+ and PO_4 fluxes. With regards to the PO_4 flux, the parameters selected by the final MLR model were the phaeopigment, Fe-P and Org-P contents, and the porosity (Figure 5). Whereas the PO_4 flux was positively and significantly correlated with the phaeopigment and Fe-P contents (p -value < 0.05), it was negatively and significantly correlated with the porosity (p -value < 0.05). In addition, a positive relationship was observed between the Org-P content and the PO_4 flux, despite a less significant effect (p -value = 0.079). To predict the NH_4^+ flux, the porosity, chl *a* content and C:N and TN:Org-P ratios in the SOM were selected by the final MLR model (Figure 6). The porosity, as well as the TN:Org-P ratio and chl *a* content, were positively correlated with the NH_4^+ flux. In contrast, a negative relationship was observed between the C:N ratio and the NH_4^+ flux. The parameter with the highest significant effect was porosity (p -value < 0.001), followed by the TN:Org-P ratio (p -value = 0.01). The chl *a* content and C:N ratio presented a less significant relationship with the NH_4^+ flux (p -value > 0.05).

The accuracy of the prediction remained low for both models, with only 18 and 24% of the NH_4^+ and PO_4 flux variations explained, respectively.

4. Discussion

In the present study, 75% of the NH_4^+ and PO_4 fluxes were below 151 and 24 $\mu\text{mol}\cdot\text{m}^{-2}\cdot\text{h}^{-1}$, respectively. These measurements were within the range found in previous studies carried out in Brittany and other

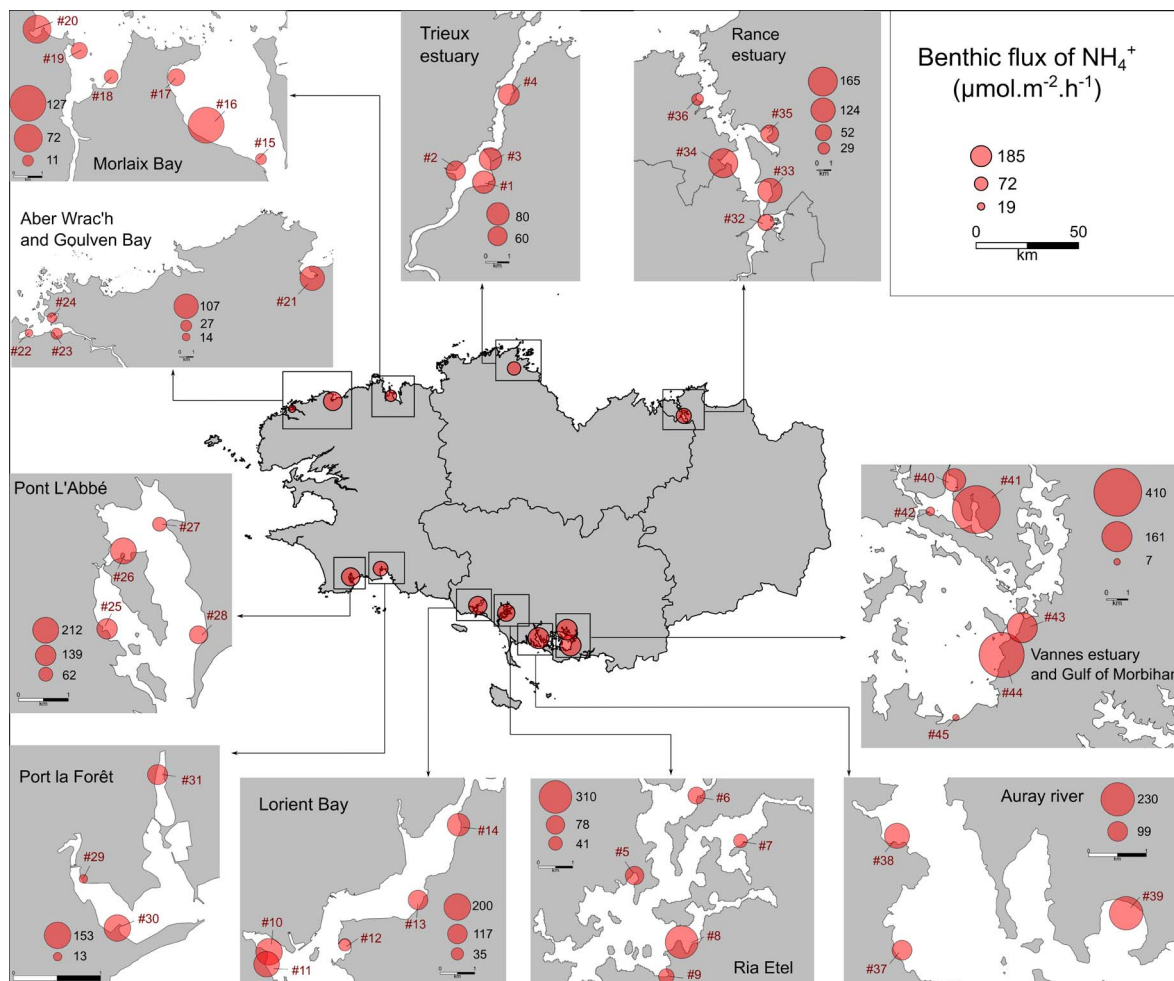


Figure 3. Spatial variability of the NH_4^+ effluxes ($\mu\text{mol}\cdot\text{m}^{-2}\cdot\text{h}^{-1}$) from the sediment collected on 45 sites in Brittany (France). The values represent the average flux of NH_4^+ for each sampling site and for each intertidal area as a whole ($n = 12$).

European intertidal mudflats during the spring period, from either incubation in the dark or porewater nutrient profiles (Table 3). Higher values were also measured in our work, reaching $526 \mu\text{mol}\cdot\text{m}^{-2}\cdot\text{h}^{-1}$ for NH_4^+ and $172 \mu\text{mol}\cdot\text{m}^{-2}\cdot\text{h}^{-1}$ for PO_4 . Significant differences in the benthic nutrient fluxes were observed between the sampling locations (Table S1). For example, the mouth of the Penzé River (sites #18 and #19) presented an average NH_4^+ flux of $25 \pm 16 \mu\text{mol}\cdot\text{m}^{-2}\cdot\text{h}^{-1}$, whereas this value was $162 \pm 132 \mu\text{mol}\cdot\text{m}^{-2}\cdot\text{h}^{-1}$ in the Auray River (sites #37, #38 and #39) (Figure 3). These results are in agreement with the NH_4^+ fluxes observed in the same areas by Lerat *et al.* [1990] and Andrieux-Loyer *et al.*

[2014] (Table 3). Thus, our broad sampling program emphasized the variability of NH_4^+ and PO_4 fluxes at the regional scale. Considering these large variations in NH_4^+ and PO_4 fluxes, using an average benthic flux on the regional scale does not seem appropriate for environmental modeling and management at a local scale. This requires the availability of data over a given area [Le Moal *et al.*, 2019], which may be facilitated by the use of proxies. In this work, we explored the possibility of using sediment characteristics for the quantification of NH_4^+ and PO_4 fluxes. These parameters were identified *via* a modeling approach using a stepwise Multiple Linear Regression (MLR). One of the questions asked here was whether or not

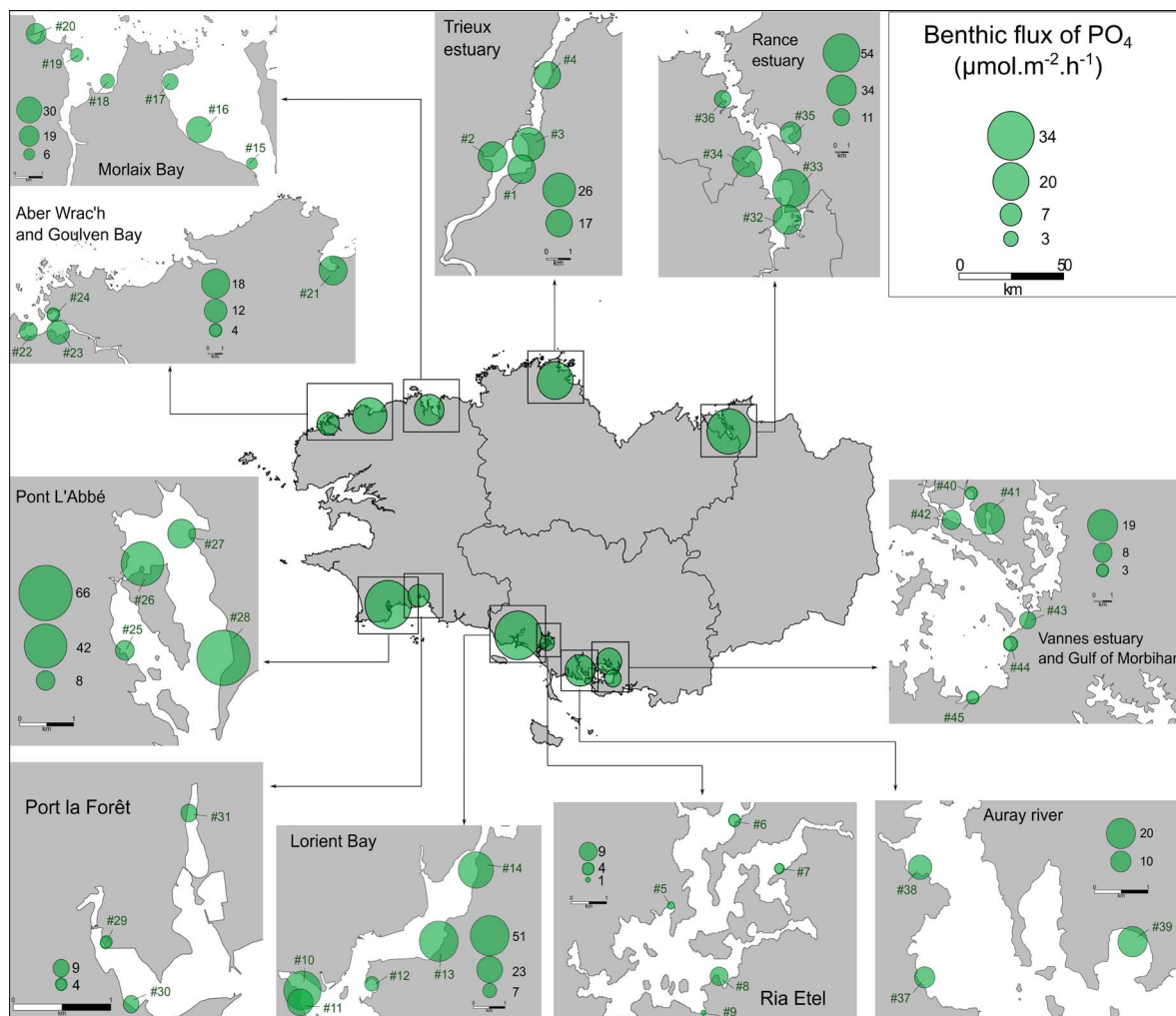


Figure 4. Spatial variability of the PO_4 effluxes ($\mu\text{mol}\cdot\text{m}^{-2}\cdot\text{h}^{-1}$) from the sediment collected on 45 sites in Brittany (France). The values represent the average flux of PO_4 for each sampling site and for each intertidal area as a whole ($n = 12$).

the benthic nutrient fluxes were controlled by the same sedimentary parameters. The present study showed no correlation between NH_4^+ and PO_4 fluxes from sediments covering a range of 200 sampling sites. The main sedimentary parameters driving the NH_4^+ fluxes were different from those driving PO_4 fluxes.

4.1. What are the main parameters of surface sediment driving the PO_4 fluxes?

Four parameters were selected *via* the final MLR model in order to predict the PO_4 fluxes: porosity,

phaeopigment content, Fe-P content and Org-P content. Among the four selected parameters, the correlation between the Org-P content and the PO_4 flux was not significant (F -test p -value > 0.05). Therefore, the porosity, phaeopigment and Fe-P contents were considered as the key variables for predicting PO_4 fluxes.

The parameter presenting the most significant positive correlation for the PO_4 fluxes was the phaeopigment content (F -test p -value = 0.002). The phaeopigment content is an indicator of algal biomass detritus in the SOM composition [Dell'Anno *et al.*, 2002, Therkildsen and Lomstein, 1993]. In the

Table 1. Sediment properties of all samples (*n* = 200)

	Mean (±sd)	Median	Min–Max	Q1–Q3
Mud [clay + silt] (%)	68.3 (±17.2)	72.6	15.4–92.8	56.2–81.9
Porosity (%)	69.8 (±10.3)	70.1	46.1–86.5	62.2–78.8
Chla (µg·g ^{−1})	5.8 (±4.8)	4.9	0–27.8	3.1–8.4
Phaeopigment (µg·g ^{−1})	28.0 (±18.7)	26.1	0–107.0	15.2–39.7
TN (%)	0.24 (±0.12)	0.22	0.06–0.64	0.15–0.32
TOC (%)	2.2 (±1.2)	2.1	0.2–7.7	1.1–3.0
C:N (mol·mol ^{−1})	10.0 (±2.4)	9.8	1.0–21.9	8.7–10.9
<i>P</i> _{tot} (%)	0.055 (±0.022)	0.051	0.011–0.131	0.038–0.070
Org-P (%)	0.026 (±0.014)	0.023	0.004–0.065	0.014–0.034
Fe-P (%)	0.008 (±0.005)	0.007	0.001–0.033	0.004–0.010
TN:Org-P (mol·mol ^{−1})	23.1 (±6.9)	22.9	5.0–65.9	19.1–25.3

Molar C:N and TN:Org-P ratios were calculated from TOC, TN and Org-P content. Q1 and Q3 represent the 25th and 75th percentile respectively.

Table 2. Pearson’s correlation matrix

	Porosity	chla	Phaeo	TN	TOC	C:N	Org-P	Fe-P	TN:Org-P
Mud	0.82	0.44	0.70	0.73	0.64	0.30	0.72	0.54	−0.20
Porosity		0.57	0.76	0.87	0.78	0.35	0.73	0.54	−0.04
chla			0.64	0.66	0.62	0.26	0.60	0.45	−0.04
Phaeo				0.86	0.79	0.31	0.70	0.53	0.04
TN					0.91	0.32	0.82	0.58	−0.02
TOC						0.66	0.75	0.58	−0.02
C:N							0.31	0.33	−0.05
Org-P								0.65	−0.48
Fe-P									−0.23

Bold values were coefficients ≥ 0.70. “mud” represents the percentage contribution of clay and silt particles (diameter < 0.63 µm). “chla”, “phaeo”, “TOC”, “TN”, “Org-P” and “Fe-P” corresponds to the content of chlorophyll a, phaeopigment, total organic carbon, total nitrogen, total phosphorus, organic phosphorus and phosphorus associated with iron oxides respectively in the upper 5 cm of sediment. Molar C:N and TN:Org-P ratios were calculated from TOC, TN and Org-P content.

present study, the significant and positive correlations between the phaeopigment content and that of the TOC, TN and Org-P contents indicated that the organic matter was enriched in the surface sediment due to the accumulation of algal detritus. In the Auray River (Brittany, France), Andrieux-Loyer *et al.* [2014] also observed that the increase in the phaeopigment, TOC, TN and Org-P contents in the

surface sediment was fueled by the occurrence of green macroalgae. An accumulation of algal OM most likely results in intense SOM mineralization, leading to both oxygen depletion in porewater and a shift in anaerobic mineralization from iron to sulfate reduction thereby enabling iron-sulfide formation [Lehtoranta *et al.*, 2009]. Under these anoxic conditions, the adsorption of PO₄ onto iron oxides would

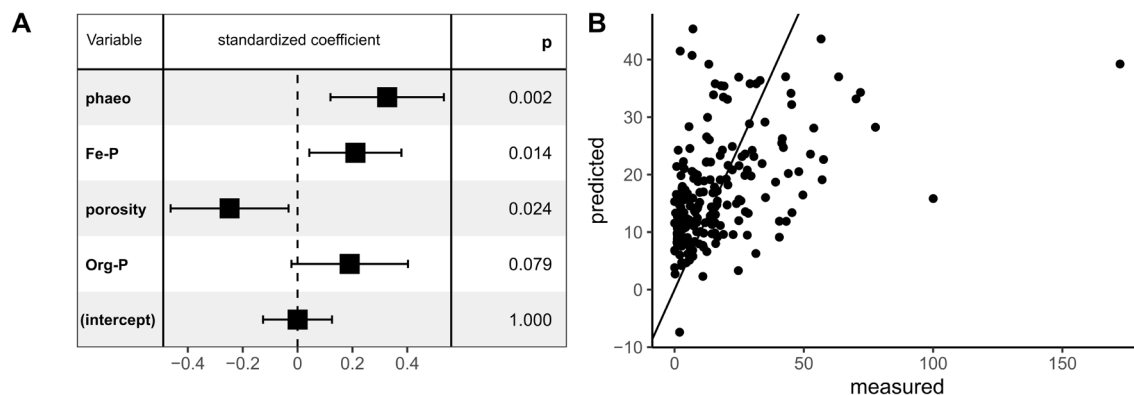


Figure 5. Parameters selected during the stepwise selection procedure by multiple linear regression (MLR) to predict PO_4 flux (A). The effect of each parameter on the model was characterized by the standardized coefficient and its significance by the p_{value} of F -test. The fitted values of PO_4 flux by the model were plotted versus PO_4 fluxes measured by core incubations ($\mu\text{mol}\cdot\text{m}^{-2}\cdot\text{h}^{-1}$) (B). The straight line represents the slope 1:1.

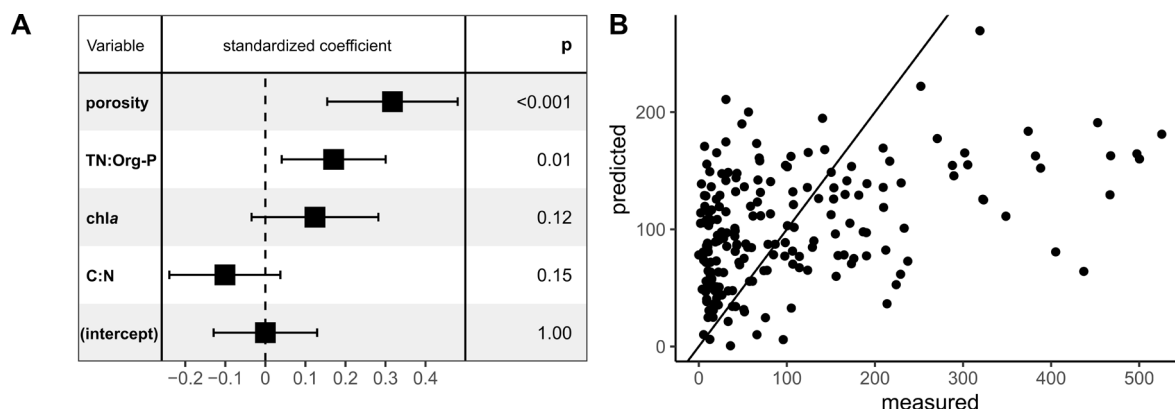


Figure 6. Parameters selected during the stepwise selection procedure by multiple linear regression (MLR) to predict NH_4^+ flux (A). The effect of each parameter on the model was characterized by the standardized coefficient and its significance by the p_{value} of F -test. The fitted values of NH_4^+ flux by the model were plotted versus NH_4^+ fluxes measured by core incubations ($\mu\text{mol}\cdot\text{m}^{-2}\cdot\text{h}^{-1}$) (B). The straight line represents the slope 1:1.

be less efficient, increasing the upward diffusion of PO_4 from the sediment [Ekholm and Lehtoranta, 2012 and references therein; Lehtoranta et al., 2009, Rozan et al., 2002]. Thus, surface sediment that is rich in algal detritus would be a more effective source of PO_4 due to the creation of anoxic conditions and the subsequent desorption of P (Figure 7A). The solubilization of Fe-P has been shown to be a main process in PO_4 release in overlying water from sulfidic

sediments during macroalgal blooms [Rozan et al., 2002]. Consequently, sediment that is rich in Fe-P would represent a potentially bioavailable source of P under anoxic conditions. This is in good agreement with our results which identify the Fe-P content as the second main driver, and which was positively correlated with the PO_4 flux.

In contrast to the previous variables, porosity, the third main driver, was negatively correlated with

Table 3. Estimations of NH_4^+ and PO_4 fluxes at sediment–water interface in the present study and from other European intertidal mudflats

Location	Method	Period	NH_4^+ flux	PO_4 flux	Reference
Brittany mudflats, France	Core incubation	Spring 2019	101 ± 117	17 ± 20	Present study
Aber Benoît, Brittany, France	Calculation from porewater profiles	May 2008	39 ± 16	<6	Andrieux-Loyer et al. [2014]
The Auray River, Brittany, France	Calculation from porewater profiles	May 2009	206 ± 47	<6	Andrieux-Loyer et al. [2014]
The Penzé River, Brittany, France	Core incubation	March 1985 July 1985	48 21	5 2	Lerat [1990]; Lerat et al. [1990]
Marennes-Oléron Bay, France	Core incubation	March 1999 June 1999	$138 \pm 75^*$ $58 \pm 25^*$		Laima et al. [2002]
Rågårdsvik and Bassholmen, Sweden	Core incubation	April–June 2000	<70	<5	Sundbäck and Miles [2002]
Palmones River, Spain	Opaque PVC benthic chamber	May 1997	$187 \pm 18^*$	$1 \pm 2^*$	Clavero et al. [2000]

All incubations were carried out in the dark. NH_4^+ and PO_4 fluxes are expressed as $\mu\text{mol}\cdot\text{m}^{-2}\cdot\text{h}^{-1}$. *When daily flux was converted into hour assuming a 24 h-period.

the PO_4 flux. An increase in porosity favors the diffusion of solutes through the sediment [Boudreau, 1996], and as a result, a positive effect on the PO_4 fluxes could be expected due to an upward diffusion from the sediment. On the other hand, high porosity may also improve the oxygen diffusion across the sediment–water interface [House, 2003]. The ferrous ion (Fe^{2+}) oxidation followed by the re-precipitation of iron oxides at the oxygenated interface, would increase the adsorption sites for PO_4 [e.g. Krom and Berner, 1980, Gunnars et al., 2002, Mayer and Jarrell, 2000, Zhang et al., 2010]. This may limit the release of PO_4 into the overlying water, thereby explaining the negative correlation between the porosity and the PO_4 flux observed in the present study.

4.2. What are the main parameters of surface sediment driving the NH_4^+ fluxes?

The parameters selected by the final MLR model for predicting the NH_4^+ fluxes were the porosity, the TN:Org-P ratio, the chl *a* content and the C:N ratio. Only the porosity and TN:Org-P ratio had a significant effect (*F*-test *p*-value < 0.05), and were thus

considered as the key variables for predicting NH_4^+ fluxes.

Contrary to the PO_4 flux, the NH_4^+ flux was positively correlated with the porosity. When sediment has a high porosity, this likely enhances the diffusion of solutes across the sediment–water interface [Boudreau, 1996] including that of NH_4^+ . As discussed above, an increase in porosity could also enhance the oxygen diffusion at the sediment–water interface. This may favor the oxidation of NH_4^+ by nitrifying microorganisms, and could therefore increase the effluxes of oxidized nitrogen species (NO_x) at the expense of NH_4^+ [Capone et al., 2008 and references therein]. In the present study, the impact of nitrification on the NH_4^+ fluxes seemed to be negligible as there was neither a negative effect of the porosity on the NH_4^+ fluxes nor a release of NO_x in the overlying water ($[\text{NO}_x] < \text{detection limit}$) (Figure 7B). Consequently, the enhanced oxygen diffusion in the upper layer of the sediment due to the increase in porosity would poorly impact the efflux of NH_4^+ in contrast to that of PO_4 . This could be explained by the fact that abiotic Fe^{2+} oxidation, fueling the precipitation of Fe-P, would be faster and less oxygen-limited compared to NH_4^+ oxidation [Canavan et al., 2006].

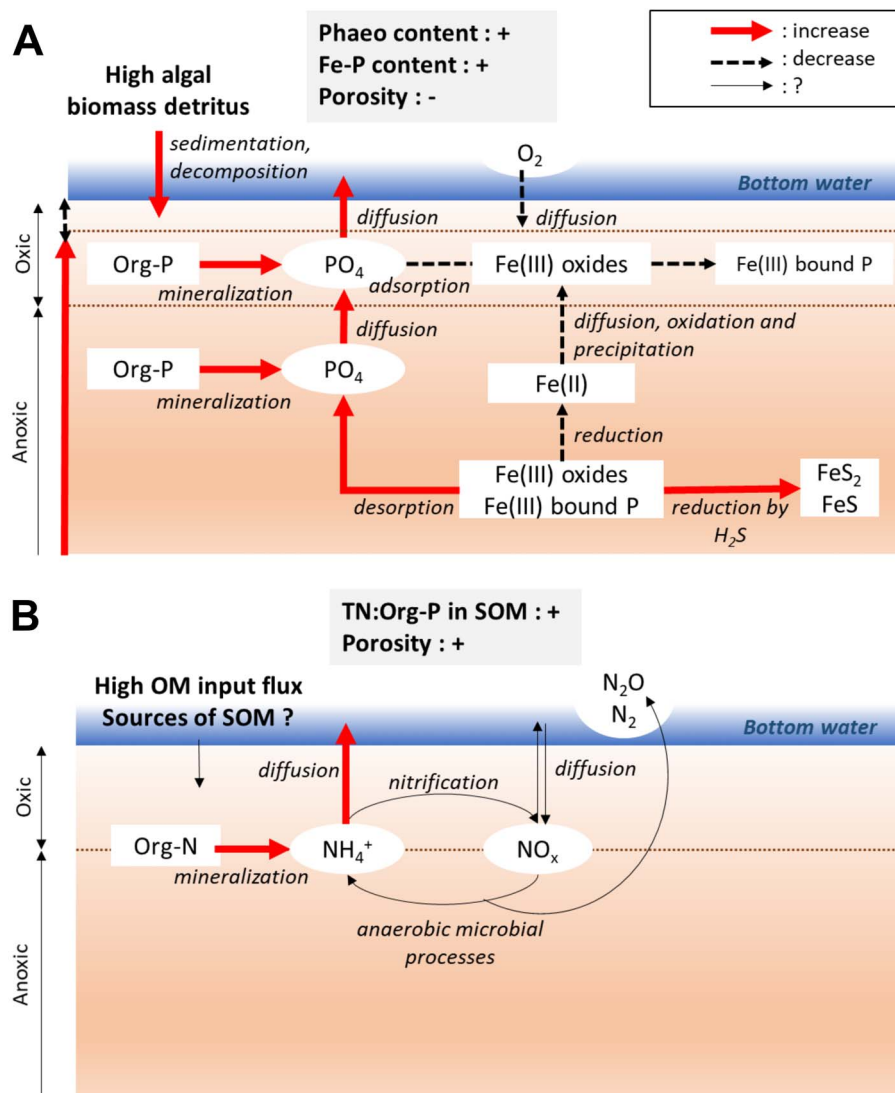


Figure 7. Stimulation of PO₄ effluxes by an increase in phaeopigment and Fe-P content, and a decrease in porosity of surface sediment. A high algal biomass detritus and a low porosity decrease the oxic surface layer of sediment, and modify the anaerobic microbial reduction. This enhances the solubilization of Fe(III)-bound P, and avoids the re-adsorption of PO₄ on Fe(III) oxides at the interface sediment–water (A). Stimulation of NH₄⁺ effluxes by an increase in TN:Org-P and porosity of surface sediment. Mineralization of SOM rich in N enhances the regeneration of NH₄⁺ in sediment. NH₄⁺ is released to overlying water by diffusion during the core incubation, which largely depends on porosity of sediment. Other changes in microbial N transformations in sediment cannot be stated here (B). Bottom water: nutrient-free and oxygenated artificial seawater used during the core incubations.

The positive correlation observed between the porosity and the NH₄⁺ flux might also be explained by the fact that the sediments with higher porosity would be also associated with higher OM input flux,

through the positive and significant correlation observed between the porosity and e.g. the TOC content (Table 2). Indeed, an increase in the deposition of OM in the sediment, supported by the river export of fine

mud particles (with higher porosity, Table 2), can improve the mineralization rates of SOM, as observed in the Elorn and Aulne estuaries in Brittany [Khalil *et al.*, 2018], and thus lead to a larger NH_4^+ regeneration in porewaters of sediment. Thereby, higher NH_4^+ recycling rates combined with higher sediment–water exchanges could enhance the diffusion of NH_4^+ to the overlying water.

In addition to the porosity, the NH_4^+ flux was significantly and positively correlated with the TN:Org-P ratio in the SOM. This suggests that the NH_4^+ fluxes were controlled by the elemental composition of the SOM. SOM that is rich in both N and easily biodegradable compounds enhances the production of NH_4^+ in the sediment *via* SOM mineralization [Capone *et al.*, 2008 and references therein], releasing NH_4^+ into the overlying water (Figure 7B). In coastal systems, the SOM composition depends on a large variability of marine and terrigenous sources of OM [e.g. Carlier *et al.*, 2008, Cook *et al.*, 2004, Dubois *et al.*, 2012]. As a result, the variability of the TN:Org-P ratio in the SOM observed in the present study may be controlled by different OM sources. An increase in the TN:Org-P ratio in the SOM ratio could indicate an accumulation of macroalgae in coastal systems. Such a relationship has been observed in the Venetian lagoon during the spring and summer [Sfriso *et al.*, 1988]. An increase in this ratio could also reflect an anthropogenic N input from riverine particulate matter. This was based on imbalances in the N:P ratio observed in watersheds in previous studies, which depend on industrial and agricultural activities, and the management policy [Arbuckle and Downing, 2001, Bouwman *et al.*, 2017, Carpenter *et al.*, 1998, Guenther *et al.*, 2015, Sardans *et al.*, 2012].

4.3. *Sedimentary proxies: a good tool to predict NH_4^+ and PO_4 fluxes?*

We hypothesized that the chl *a* content and the C:N ratio, i.e. tracers of labile OM input fluxes explain the spatial variability in benthic nutrient fluxes and therefore allowing them to be used as proxies. Such correlations between these two parameters and the NH_4^+ and PO_4 fluxes were shown by Cowan and Boynton [1996] and Clavero *et al.* [2000]. In the present study, the chl *a* content and the C:N ratio were selected by the final MLR model of the NH_4^+ flux,

but without significant correlations (*F*-test *p*-value > 0.05). With regard to the PO_4 fluxes, the modeling approach did not identify the chl *a* content and the C:N ratio as main drivers. However, other parameters related to the SOM composition presented significant correlations with the benthic nutrient fluxes: i.e. the TN:Org-P ratio for the NH_4^+ flux, and the phaeopigment content, a chl *a* breakdown product, for the PO_4 flux. The characterization of SOM composition, largely dependent on the spatial variability of OM sources, may require more specific tools (e.g. isotopic or biomolecular markers) to better relate the benthic nutrient fluxes to the sedimentary composition.

In the present study, the stepwise MLR allowed to select the best combinations of parameters to predict NH_4^+ and PO_4 fluxes. Nevertheless, only 18 and 24% of NH_4^+ and PO_4 flux variations respectively were explained by our modeling approach. This highlights the difficulty to determine the controls on the benthic nutrient fluxes by sedimentary proxies in the intertidal mudflats at the regional scale where the rate deposition of particulate matter is influenced by river discharges, tidal fluctuations and anthropogenic pressures [Bauer *et al.*, 2013].

In addition, the contribution of biological parameters was not considered in the present work, which could explain the weak accuracy of prediction for both models of NH_4^+ and PO_4 fluxes. The NH_4^+ and PO_4 fluxes may be impacted by bioturbation, through particle reworking and burrow ventilation by the benthic macrofauna [Kristensen *et al.*, 2012]. Bioturbation enhances the solute exchanges between the porewater and the overlying water, affects the remobilization of burial OM, and modifies the redox conditions [Graf and Rosenberg, 1997, Welsh, 2003, Kristensen *et al.*, 2012]. The stimulation of NH_4^+ and PO_4 fluxes varies according to the density, the burrowing depth, the ventilation of the benthic macrofauna, and the specific-site conditions (e.g. sediment components, nutrient concentrations in porewater). The study carried out in four European estuaries by Nizzoli *et al.* [2007] has shown that the early stage of sediment colonization by the polychaete *Nereis* spp. stimulated the NH_4^+ effluxes in all geographical areas (from 1.5 to 4-fold higher) and promoted the sediment to act either as a sink or a source of PO_4 according to the site-specific conditions. This thus leads to shifts in the magnitude of effluxes and ratios of N:P

fluxes which depend on the spatial variability of environmental conditions.

5. Conclusion

The broad sediment sampling carried out at the regional scale in the present study has allowed to determine the main parameters of the surface sediment driving the NH_4^+ and PO_4 fluxes. The results have shown that (1) high phaeopigment and iron-bound phosphorus (Fe-P) contents and a low porosity were related to a high PO_4 flux, and (2) a high porosity and TN:Org-P ratio in the SOM were related to a high NH_4^+ flux. The PO_4 fluxes would be more driven by the redox status of the sediment through the desorption of Fe-P under specific anoxic conditions during the algal decomposition. The NH_4^+ fluxes would be more driven by high NH_4^+ recycling rates from SOM mineralization and high sediment–water exchanges, enhancing the diffusion of NH_4^+ to the overlying water. The present work has highlighted that the interactions between the SOM composition and physical properties in the sediment exert a control on the benthic fluxes. This reflects the connections between the microbial (SOM mineralization), chemical (adsorption–desorption) and physical (diffusion) processes (Figure 7). We focussed on the surface sediment characteristics in order to assess the pertinence of these parameters for use as proxies of the NH_4^+ and PO_4 fluxes. It has underlined that the NH_4^+ and PO_4 fluxes are partially explained by these sedimentary parameters, and we suggest that the spatial variability of the biological parameters should be considered in future investigations. In addition, in order to better understand the effect of SOM on benthic nutrient fluxes, the sources of OM in the sediment need to be better discerned in a future work using stable isotope and biomolecular analysis.

Acknowledgments

This work was funded by Loire-Bretagne Water Agency and the Regional Council of Brittany (France). It was carried out as a part of the IMPRO research project. The authors would like to thank O. Jambon and C. Roose-Amsaleg for their assistance in the field. The CEVA, the Syndicat Mixte EPTB Rance-Fremur, the Pays de Guingamp, the Syndicat Mixte des Bassins du Haut-Léon, the Syndicat des

Eaux du Bas-Léon, Lorient-Agglomération, the Syndicat Mixte du SAGE Ouest-Cornouaille (OUESCO), Concarneau-Cornouaille-Agglomération, the Syndicat Mixte de la Ria d'Étel (SMRE) and the Syndicat Mixte du Loc'h et du Sal (SMLS) are acknowledged for their help in preparing the field campaign. The authors would also like to thank O. Lebeau (Plateforme Isotopes Stables, IUEM) and Marie-Claire Perello (EPOC, University of Bordeaux) for the elemental and particle-size analyses, respectively. S. Mullin is acknowledged for carefully checking the English content. The authors would also like to thank C. Rabouille for his constructive comments and suggestions in order to improve the quality of the paper.

Supplementary data

Supporting information for this article is available on the journal's website under <https://doi.org/10.5802/crgeos.57> or from the author.

References

- Ait Ballagh, F. E., Rabouille, C., Andrieux-Loyer, F., Soetaert, K., Elkalay, K., and Khalil, K. (2020). Spatio-temporal dynamics of sedimentary phosphorus along two temperate eutrophic estuaries: A data-modelling approach. *Cont. Shelf Res.*, 193, article no. 104037.
- Aller, R. C., Mackin, J. E., Ullman, W. J., Wang, C.-H., Tsai, S.-M., Jin, J.-C., Sui, Y.-N., and Hong, J.-Z. (1985). Early chemical diagenesis, sediment-water solute exchange, and storage of reactive organic matter near the mouth of the Changjiang, East China Sea. *Cont. Shelf Res.*, 4, 227–251.
- Aminot, A. and Kérouel, R. (2007). Dosage automatique des nutriments dans les eaux marines : Automated determination of nutrients in marine waters. In *Méthodes d'analyse en milieu marin*, page 188. Ifremer.
- Andrieux-Loyer, F., Azandegbé, A., Caradec, F., Philippon, X., Kérouel, R., Youenou, A., and Nicolas, J.-L. (2014). Impact of Oyster farming on diagenetic processes and the phosphorus cycle in two estuaries (Brittany, France). *Aquat. Geochem.*, 20, 573–611.
- Andrieux-Loyer, F., Philippon, X., Bally, G., Kérouel, R., Youenou, A., and Le Grand, J. (2008). Phosphorus dynamics and bioavailability in sediments

- of the Penzé Estuary (NW France): in relation to annual P-fluxes and occurrences of Alexandrium Minutum. *Biogeochemistry*, 88, 213–231.
- Arbuckle, K. E. and Downing, J. A. (2001). The influence of watershed land use on lake N: P in a predominantly agricultural landscape. *Limnol. Oceanogr.*, 46, 970–975.
- Arndt, S., Jørgensen, B. B., LaRowe, D. E., Middelburg, J. J., Pancost, R. D., and Regnier, P. (2013). Quantifying the degradation of organic matter in marine sediments: A review and synthesis. *Earth Sci. Rev.*, 123, 53–86.
- Aspila, K., Agemian, H. Y., and Chau, A. S. (1976). A semi-automated method for the determination of inorganic, organic and total phosphate in sediments. *Analyst*, 101, 187–197.
- Bauer, J. E., Cai, W.-J., Raymond, P. A., Bianchi, T. S., Hopkinson, C. S., and Regnier, P. A. G. (2013). The changing carbon cycle of the coastal ocean. *Nature*, 504, 61–70.
- Boudreau, B. P. (1996). A method-of-lines code for carbon and nutrient diagenesis in aquatic sediments. *Comput. Geosci.*, 22, 479–496.
- Boudreau, B. P. (1997). *Diagenetic Models and Their Implementation: Modelling Transport and Reactions in Aquatic Sediments*. Springer, Berlin, Heidelberg.
- Bouwman, A. F., Beusen, A. H. W., Lassaletta, L., van Apeldoorn, D. F., van Grinsven, H. J. M., Zhang, J., and van Ittersum, M. K. (2017). Lessons from temporal and spatial patterns in global use of N and P fertilizer on cropland. *Sci. Rep.*, 7, article no. 40366.
- Canavan, R. W., Slomp, C. P., Jourabchi, P., Van Cappellen, P., Laverman, A. M., and van den Berg, G. A. (2006). Organic matter mineralization in sediment of a coastal freshwater lake and response to salinization. *Geochim. Cosmochim. Acta*, 70, 2836–2855.
- Capone, D. G., Bronk, D. A., Mulholland, M. R., and Carpenter, E. J. (2008). *Nitrogen in the Marine Environment*. Elsevier.
- Carrier, A., Riera, P., Amouroux, J.-M., Bodiou, J.-Y., Desmalades, M., and Grémare, A. (2008). Food web structure of two Mediterranean lagoons under varying degree of eutrophication. *J. Sea Res.*, 60, 264–275.
- Carpenter, S. R., Caraco, N. F., Correll, D. L., Howarth, R. W., Sharpley, A. N., and Smith, V. H. (1998). Non-point pollution of surface waters with phosphorus and nitrogen. *Ecol. Appl.*, 8, 559–568.
- CEVA (2015). Contribution du sédiment aux cycles de l'Azote et du Phosphore en zone côtière – Impacts potentiels sur les marées vertes. Annexe au rapport 2014 du projet 1 du programme CIMAV 62.
- Clavero, V., Izquierdo, J., Fernández, J., and Niell, F. (2000). Seasonal fluxes of phosphate and ammonium across the sediment-water interface in a shallow small estuary (Palmones River, southern Spain). *Mar. Ecol. Prog. Ser.*, 198, 51–60.
- Cook, P., Revill, A., Clementson, L., and Volkman, J. (2004). Carbon and nitrogen cycling on intertidal mudflats of a temperate Australian estuary. III. Sources of organic matter. *Mar. Ecol. Prog. Ser.*, 280, 55–72.
- Cowan, J. L. W. and Boynton, W. R. (1996). Sediment-water oxygen and nutrient exchanges along the longitudinal axis of Chesapeake Bay: seasonal patterns, controlling factors and ecological significance. *Estuaries*, 19, 562–580.
- Dauwe, B., Middelburg, J., and Herman, P. (2001). Effect of oxygen on the degradability of organic matter in subtidal and intertidal sediments of the North Sea area. *Mar. Ecol. Prog. Ser.*, 215, 13–22.
- Davoult, D., Surget, G., Stiger-Pouvreau, V., Noiset, F., Riera, P., Stagnol, D., Androuin, T., and Poupart, N. (2017). Multiple effects of a Gracilaria vermiculophylla invasion on estuarine mudflat functioning and diversity. *Mar. Environ. Res.*, 131, 227–235.
- Dell'Anno, A., Mei, M. L., Pusceddu, A., and Danovaro, R. (2002). Assessing the trophic state and eutrophication of coastal marine systems: a new approach based on the biochemical composition of sediment organic matter. *Mar. Pollut. Bull.*, 44, 611–622.
- Dubois, S., Savoye, N., Grémare, A., Plus, M., Charlier, K., Beltoise, A., and Blanchet, H. (2012). Origin and composition of sediment organic matter in a coastal semi-enclosed ecosystem: An elemental and isotopic study at the ecosystem space scale. *J. Mar. Syst.*, 94, 64–73.
- Ekholm, P. and Lehtoranta, J. (2012). Does control of soil erosion inhibit aquatic eutrophication? *J. Environ. Manage.*, 93, 140–146.
- Engelsen, A., Hulth, S., Pihl, L., and Sundbäck, K. (2008). Benthic trophic status and nutrient fluxes in shallow-water sediments. *Estuar. Coast. Shelf Sci.*, 78, 783–795.

- Enríquez, S., Duarte, C. M., and Sand-Jensen, K. (1993). Patterns in decomposition rates among photosynthetic organisms: the importance of detritus C:N:P content. *Oecologia*, 94, 457–471.
- Flemming, B. W. (2000). A revised textural classification of gravel-free muddy sediments on the basis of ternary diagrams. *Cont. Shelf Res.*, 20, 1125–1137.
- Galois, R., Blanchard, G., Seguignes, M., Huet, V., and Joassard, L. (2000). Spatial distribution of sediment particulate organic matter on two estuarine intertidal mudflats: a comparison between Marennes-Oléron Bay (France) and the Humber Estuary (UK). *Cont. Shelf Res.*, 20, 1199–1217.
- García-Robledo, E., Corzo, A., de Lomas, J., and van Bergeijk, S. (2008). Biogeochemical effects of macroalgal decomposition on intertidal microbenthos: a microcosm experiment. *Mar. Ecol. Prog. Ser.*, 356, 139–151.
- Gladyshev, M. I. and Gubelit, Y. I. (2019). Green tides: new consequences of the eutrophication of natural waters (invited review). *Contemp. Probl. Ecol.*, 12, 109–125.
- Graf, G. and Rosenberg, R. (1997). Bioresuspension and biodeposition: a review. *J. Mar. Syst.*, 11, 269–278.
- Gu, Y.-G., Ouyang, J., Ning, J.-J., and Wang, Z.-H. (2017). Distribution and sources of organic carbon, nitrogen and their isotopes in surface sediments from the largest mariculture zone of the eastern Guangdong coast, South China. *Mar. Pollut. Bull.*, 120, 286–291.
- Guenther, M., Araújo, M., Flores-Montes, M., Gonzalez-Rodriguez, E., and Neumann-Leitão, S. (2015). Eutrophication effects on phytoplankton size-fractionated biomass and production at a tropical estuary. *Mar. Pollut. Bull.*, 91, 537–547.
- Gunnars, A., Blomqvist, S., Johansson, P., and Andersson, C. (2002). Formation of Fe(III) oxyhydroxide colloids in freshwater and brackish seawater, with incorporation of phosphate and calcium. *Geochim. Cosmochim. Acta*, 66, 745–758.
- Hardison, A. K., Canuel, E. A., Anderson, I. C., Tobias, C. R., Veuger, B., and Waters, M. N. (2013). Microphytobenthos and benthic macroalgae determine sediment organic matter composition in shallow photic sediments. *Biogeosciences*, 10, 5571–5588.
- House, W. A. (2003). Factors influencing the extent and development of the oxic zone in sediments. *Biogeochemistry*, 63, 317–334.
- Keil, R. G. and Hedges, J. I. (1993). Sorption of organic matter to mineral surfaces and the preservation of organic matter in coastal marine sediments. *Chem. Geol.*, 107, 385–388.
- Khalil, K., Laverman, A. M., Raimonet, M., and Rabouille, C. (2018). Importance of nitrate reduction in benthic carbon mineralization in two eutrophic estuaries: modeling, observations and laboratory experiments. *Mar. Chem.*, 199, 24–36.
- Kristensen, E., Penha-Lopes, G., Delefosse, M., Valdemarsen, T., Quintana, C., and Banta, G. (2012). What is bioturbation? The need for a precise definition for fauna in aquatic sciences. *Mar. Ecol. Prog. Ser.*, 446, 285–302.
- Krom, M. D. and Berner, R. A. (1980). Adsorption of phosphate in anoxic marine sediments: Adsorption of phosphate. *Limnol. Oceanogr.*, 25, 797–806.
- Laima, M., Brossard, D., Sauriau, P.-G., Girard, M., Richard, P., Gouleau, D., and Joassard, L. (2002). The influence of long emersion on biota, ammonium fluxes and nitrification in intertidal sediments of Marennes-Oléron Bay, France. *Mar. Environ. Res.*, 53, 381–402.
- Le Moal, M., Gascuel-Oudou, C., Ménesguen, A., Souchon, Y., Étrillard, C., Levain, A., Moatar, F., Pannard, A., Souchu, P., Lefebvre, A., and Pinay, G. (2019). Eutrophication: A new wine in an old bottle? *Sci. Total Environ.*, 651, 1–11.
- Lehtoranta, J., Ekholm, P., and Pitkänen, H. (2009). Coastal eutrophication thresholds: a matter of sediment microbial processes. *AMBIO: A J. Human Environ.*, 38, 303–308.
- Lerat, Y. (1990). Cycles annuels de la matière organique et des éléments nutritifs dans les sédiments d'un écosystème côtier (baie de Morlaix, France) interactions avec le compartiment pélagique. Thèse de Doctorat en Chimie Marine, Université de Bretagne Occidentale. Brest.
- Lerat, Y., Lasserre, P., and le Corre, P. (1990). Seasonal changes in pore water concentrations of nutrients and their diffusive fluxes at the sediment-water interface. *J. Exp. Mar. Biol. Ecol.*, 135, 135–160.
- Liénart, C., Savoye, N., Bozec, Y., Breton, E., Conan, P., David, V., Feunteun, E., Grangeré, K., Kerhervé, P., Lebreton, B., Lefebvre, S., L'Helguen, S., Mousseau,

- L., Raimbault, P., Richard, P., Riera, P., Sauriau, P.-G., Schaal, G., Aubert, F., Aubin, S., Bichon, S., Boinet, C., Bourasseau, L., Bréret, M., Caparros, J., Cariou, T., Charlier, K., Claquin, P., Cornille, V., Corre, A.-M., Costes, L., Crispi, O., Crouvoisier, M., Czamanski, M., Del Amo, Y., Derriennic, H., Dindinaud, F., Durozier, M., Hanquiez, V., Nowaczyk, A., Devesa, J., Ferreira, S., Fornier, M., Garcia, F., Garcia, N., Geslin, S., Grossteffan, E., Gueux, A., Guillaumeau, J., Guillou, G., Joly, O., Lachaussee, N., Lafont, M., Lamoureux, J., Lecuyer, E., Lehodey, J.-P., Lemeille, D., Leroux, C., Macé, E., Maria, E., Pineau, P., Petit, F., Pujo-Pay, M., Rimelin-Maury, P., and Sultan, E. (2017). Dynamics of particulate organic matter composition in coastal systems: A spatio-temporal study at multi-systems scale. *Prog. Oceanogr.*, 156, 221–239.
- Lorenzen, C. J. (1967). Determination of chlorophyll and pheo-pigments: spectrophotometric equations 1. *Limnol. Oceanogr.*, 12, 343–346.
- Mayer, T. D. and Jarrell, W. M. (2000). Phosphorus sorption during iron(II) oxidation in the presence of dissolved silica. *Water Res.*, 34, 3949–3956.
- Meade, R. H. (1966). Factors influencing the early stages of the compaction of clays and sands—review. *SEPM JSR*, 36. <https://doi.org/10.1306/74D71604-2B21-11D7-8648000102C1865D>.
- Ménesguen, A., Dussauze, M., Dumas, F., Thouvenin, B., Garnier, V., Lecornu, F., and Répécaud, M. (2019). Ecological model of the Bay of Biscay and English Channel shelf for environmental status assessment part 1: Nutrients, phytoplankton and oxygen. *Ocean Model.*, 133, 56–78.
- Meyers, P. A. (1994). Preservation of elemental and isotopic source identification of sedimentary organic matter. *Chem. Geol.*, 114, 289–302.
- Middelburg, J., Klaver, G., Nieuwenhuize, J., Wielemaaker, A., de Haas, W., Vlug, T., and van der Nat, J. (1996). Organic matter mineralization in intertidal sediments along an estuarine gradient. *Mar. Ecol. Prog. Ser.*, 132, 157–168.
- Morand, P. and Briand, X. (1996). Excessive growth of macroalgae: a symptom of environmental disturbance. *Botanica Marina*, 39, 491–516.
- Nedergaard, R. I., Risgaard-Petersen, N., and Finster, K. (2002). The importance of sulfate reduction associated with *Ulva lactuca* thalli during decomposition: a mesocosm experiment. *J. Exp. Mar. Biol. Ecol.*, 275, 15–29.
- Nizzoli, D., Bartoli, M., Cooper, M., Welsh, D. T., Underwood, G. J. C., and Viaroli, P. (2007). Implications for oxygen, nutrient fluxes and denitrification rates during the early stage of sediment colonisation by the polychaete *Nereis* spp. in four estuaries. *Estuar. Coast. Shelf Sci.*, 75, 125–134.
- Paytan, A. and McLaughlin, K. (2007). The oceanic phosphorus cycle. *Chem. Rev.*, 107, 563–576.
- Perrot, T., Rossi, N., Ménesguen, A., and Dumas, F. (2014). Modelling green macroalgal blooms on the coasts of Brittany, France to enhance water quality management. *J. Mar. Syst.*, 132, 38–53.
- Pinay, G., Gascuel, C., Ménesguen, A., Souchon, Y., Moal, M. L., Levain, A., Étrillard, C., Moatar, F., Pannard, A., and Souchu, P. (2018). *L'eutrophisation: Manifestations, causes, conséquences et prédictibilité*. Editions Quae.
- Pye, K. and Blott, S. J. (2004). Particle size analysis of sediments, soils and related particulate materials for forensic purposes using laser granulometry. *Forensic Sci. Int.*, 144, 19–27.
- Rasheed, M., Badran, M. I., and Huettel, M. (2003). Influence of sediment permeability and mineral composition on organic matter degradation in three sediments from the Gulf of Aqaba, Red Sea. *Estuar. Coast. Shelf Sci.*, 57, 369–384.
- Robertson, B. P. and Savage, C. (2018). Mud-entrained macroalgae utilise porewater and overlying water column nutrients to grow in a eutrophic intertidal estuary. *Biogeochemistry*, 139, 53–68.
- Rozan, T. F., Taillefert, M., Trouwborst, R. E., Glazer, B. T., Ma, S., Herszage, J., Valdes, L. M., Price, K. S., and Luther III, G. W. (2002). Iron-sulfur-phosphorus cycling in the sediments of a shallow coastal bay: Implications for sediment nutrient release and benthic macroalgal blooms. *Limnol. Oceanogr.*, 47, 1346–1354.
- Ruttenberg, K. C. (1992). Development of a sequential extraction method for different forms of phosphorus in marine sediments. *Limnol. Oceanogr.*, 37, 1460–1482.
- Sardans, J., Rivas-Ubach, A., and Peñuelas, J. (2012). The C:N:P stoichiometry of organisms and ecosystems in a changing world: A review and perspectives. *Perspect. Plant Ecol. Evol. Syst.*, 14, 33–47.
- Sfriso, A., Pavoni, B., Marcomini, A., and Orio, A. A. (1988). Annual variations of nutrients in the Lagoon of Venice. *Mar. Pollut. Bull.*, 19, 54–60.

- Smith, V. H., Tilman, G. D., and Nekola, J. C. (1999). Eutrophication: impacts of excess nutrient inputs on freshwater, marine, and terrestrial ecosystems. *Environ. Pollut.*, 100, 179–196.
- Sundbäck, K. and Miles, A. (2002). Role of microphytobenthos and denitrification for nutrient turnover in embayments with floating macroalgal mats: a spring situation. *Aquat. Microb. Ecol.*, 30, 91–101.
- Sundbäck, K., Miles, A., Hulth, S., Pihl, L., Engström, P., Selander, E., and Svenson, A. (2003). Importance of benthic nutrient regeneration during initiation of macroalgal blooms in shallow bays. *Mar. Ecol. Prog. Ser.*, 246, 115–126.
- Sundby, B., Gobeil, C., Silverberg, N., and Alfonso, M. (1992). The phosphorus cycle in coastal marine sediments. *Limnol. Oceanogr.*, 37, 1129–1145.
- Therkildsen, M. S. and Lomstein, B. A. (1993). Seasonal variation in net benthic C-mineralization in a shallow estuary. *FEMS Microbiol. Ecol.*, 12, 131–142.
- Valiela, I., McClelland, J., Hauxwell, J., Behr, P. J., Hersh, D., and Foreman, K. (1997). Macroalgal blooms in shallow estuaries: controls and ecophysiological and ecosystem consequences. *Limnol. Oceanogr.*, 42, 1105–1118.
- Welsh, D. T. (2003). It's a dirty job but someone has to do it: The role of marine benthic macrofauna in organic matter turnover and nutrient recycling to the water column. *Chem. Ecol.*, 19, 321–342.
- Zhang, L., Gu, X., Fan, C., Shang, J., Shen, Q., Wang, Z., and Shen, J. (2010). Impact of different benthic animals on phosphorus dynamics across the sediment-water interface. *J. Environ. Sci.*, 22, 1674–1682.